

Article

Mössbauer Spectroscopy Studies on Magnetic Properties for ^{57}Fe -substituted Ni-Mn-Sn Metamagnetic Shape Memory Alloys

Rie Y. Umetsu ^{1,*}, Kenji Sano ², Kouji Fukushima ², Takeshi Kanomata ^{3,4}, Yusuke Taniguchi ⁵, Yasushi Amako ⁵ and Ryosuke Kainuma ⁶

¹ Institute for Materials Research, Tohoku University, Sendai 980-8577, Japan; Japan Science and Technology Agency-Precursory Research for Embryonic Science and Technology (JST-PREST), Tokyo 102-0076, Japan

² Faculty of Engineering, Tohoku Gakuin University, Tagajo 985-8537, Japan;
E-Mails: cofecrsi315@yahoo.co.jp (K.S.); maruhatu1@yahoo.co.jp (K.F.)

³ Research Institute for Engineering and Technology, Tohoku Gakuin University, Tagajo 985-8537, Japan; E-Mail: kanomata@tjcc.tohoku-gakuin.ac.jp

⁴ Department of Materials Science, Graduate School of Engineering, Tohoku University, Sendai 980-8579, Japan

⁵ Faculty of Science, Shinshu University, Matsumoto 390-8621, Japan;
E-Mails: taniguchi-yuusuke@hitachi-nico.jp (Y.T.); tenjine@shinshu-u.ac.jp (Y.A.)

⁶ Department of Materials Science, Graduate School of Engineering, Tohoku University, Sendai 980-8579, Japan; E-Mail: kainuma@material.tohoku.ac.jp

* Author to whom correspondence should be addressed; E-Mail: rieume@imr.tohoku.ac.jp;
Tel.: +81-22-215-2492; Fax: +81-22-215-2381.

Received: 10 April 2013; in revised form: 20 May 2013 / Accepted: 23 May 2013 /

Published: 3 June 2013

Abstract: In order to investigate the Fe substituted effects on the magnetic properties of the Ni-Mn-Sn metamagnetic shape memory alloys, magnetization and the Mössbauer spectroscopy measurements were carried out with using ^{57}Fe -doped specimens of $\text{Ni}_2\text{Mn}_{1.48-x}\text{Fe}_x\text{Sn}_{0.52}$ ($x = 0.02, 0.04$ and 0.08). Singlet-type Mössbauer spectra were clearly observed for $x = 0.02$ and 0.04 just below the martensitic transformation temperature, T_M , and above the Curie temperature, T_C , in the austenite phase. It was clear that the magnetic state in the martensite phase just below T_M was paramagnetic for $x = 0.02$ and 0.04 . In further doped ^{57}Fe to $\text{Ni}_2\text{Mn}_{1.48}\text{Sn}_{0.52}$, T_C in the austenite phase slightly increased. However, the value of T_M significantly decreased. As a result, martensite phase with small spontaneous magnetization directly transformed to the ferromagnetic austenite

phase during heating for $x = 0.08$. These results obtained from the Mössbauer spectra were consistent with the results of the magnetic measurements in this study and the phase diagram reported by Fukushima *et al.* for normal Fe-doped $\text{Ni}_2\text{Mn}_{1.48-x}\text{Fe}_x\text{Sn}_{0.52}$ alloys. The breakdown of the general rule, in which the ferromagnetic shape memory alloys with larger value of the valence electrons per atom, e/a , showed higher T_M , was also appeared in $\text{Ni}_2\text{Mn}_{1.48-x}\text{Fe}_x\text{Sn}_{0.52}$ alloys, being similar to $\text{Ni}_2\text{Mn}_{1-x}\text{Fe}_x\text{Ga}$ alloys.

Keywords: metamagnetic shape memory alloy; mössbauer spectroscopy; heusler alloy; martensitic transformation; austenite phase

1. Introduction

Ferromagnetic shape memory alloys (FSMAs) have become very attractive candidates for high performance magnetic actuator materials because they show a large magnetic-field-induced strain by the rearrangement of twin variants in the martensite phase [1,2]. Ni_2MnGa has the cubic $L2_1$ -type Heusler structure at room temperature, and orders ferromagnetically at the Curie temperature, T_C , of 365 K. On cooling below a martensitic transformation temperature, T_M , of about 200 K, a superstructure forms [3]. A number of investigations on Ni-Mn-Ga FSMAs have been described in the literature because T_C and T_M can be tuned by changing the constituent elements of Ni, Mn and Ga. Many topics relating to the Ni-Mn-Ga FSMAs have been reviewed by Entel *et al.* [4] and Brown *et al.* [5] in recent articles.

In 2004, Sutou *et al.* found new series of FSMAs, such as Ni-Mn-Z ($Z = \text{In, Sn, Sb}$) alloys, which show a drastic change of magnetization due to the martensitic transformation, MT, in where the magnetization of the martensite phase is considerably smaller than that of the austenite phase [6]. In contrast to the Ni-Mn-Ga FSMAs, where MT occurs from ferromagnetic austenite phase to ferrimagnetic martensite phase, the magnetization in the Ni-Mn-Z alloys drastically changes associated with the transformation because the magnetization is low in the martensite phase. The value of T_M of Ni-Mn-Z alloys and its Co-substituted series is significantly decreased by applied magnetic field; therefore, the magnetic-field-induced reverse MT has been confirmed below T_M [7–9]. Umetsu *et al.* have investigated Mössbauer spectroscopy in ^{57}Fe -doped $\text{Ni}_2\text{Mn}_{1.48}\text{Sn}_{0.52}$ and reported that the magnetic feature of the martensite phase just below the transformation temperature is paramagnetic [10]. Subsequently, it has also been confirmed that the martensite phase of ^{57}Fe substituted $\text{Ni}_2\text{Mn}_{1.392}\text{In}_{0.608}$ is paramagnetic by Khovaylo *et al.* [11]. These results became one of powerful key to clarify the mechanism of MT for these FSMAs.

Kikuchi *et al.* and Fukushima *et al.* have reported the phase diagrams of $\text{Ni}_2(\text{Fe,Mn})\text{Ga}$ and $\text{Ni}_2(\text{Fe,Mn})_{1.48}\text{Sn}_{0.52}$ FSMAs, respectively [12,13]. Substitution of Fe for Mn has to be known to enhance the ductility of Ni-Mn-Ga and Ni-Mn-Sn alloys, and the way is significantly effective for the applications [14,15]. Furthermore, the phase diagrams of $\text{Ni}_2(\text{Mn,Fe})\text{Ga}$ and $\text{Ni}_2(\text{Mn,Fe})_{1.48}\text{Sn}_{0.52}$ open question to behavior of the concentration dependence of T_M because it has been thought that the variation of T_M follows the general rule related to the number of the valence electrons. That is, T_M increases with increasing the number of the valence electrons per atoms, e/a , [16,17]. There have been

many reports on the variation of T_M on e/a for many kinds of FSMAs, such as Ni-Mn-Ga, Ni-Mn-Z ($Z = \text{In, Sn, Sb}$), and their element doping systems [18–21]. In these systematic studies, it has been pointed out that the behavior of T_M on e/a is different only for the Fe-doping system. Fe substitution for Mn in Ni_2MnGa and $\text{Ni}_2\text{Mn}_{1.48}\text{Sn}_{0.52}$ FSMAs increases e/a , however, T_M decreases with increasing the Fe content in both Ni_2MnGa and $\text{Ni}_2\text{Mn}_{1.48}\text{Sn}_{0.52}$ FSMAs [11,12]. Clarifying the role of the Fe substitution in Ni-Mn-Ga and Ni-Mn-Sn FSMAs is very important from the both aspects of the applications and academics. In our previous study for the Mössbauer spectroscopy in ^{57}Fe -doped $\text{Ni}_2\text{Mn}_{1.48}\text{Sn}_{0.52}$, only 0.5 at.% of ^{57}Fe was doped. In this study, we first establish that the magnetic properties of ^{57}Fe doped $\text{Ni}_2\text{Mn}_{1.48}\text{Sn}_{0.52}$ system follows the reported phase diagram for the normal Fe-doped system. Furthermore, we report the experimental results of Mössbauer spectroscopy measurements for $\text{Ni}_2\text{Mn}_{1.48}\text{Sn}_{0.52}$ FSMA with various ^{57}Fe contents. It is clear that information of this type is essential to an understanding of the mechanism of the magnetic-field-induced reverse MT observed on Ni-Mn-Sn FSMAs.

2. Experimental Section

Polycrystalline samples of $\text{Ni}_2\text{Mn}_{1.48-x}\text{Fe}_x\text{Sn}_{0.52}$ ($x = 0.02, 0.04$ and 0.08) alloys were prepared by repeated arc-melting of the appropriate quantities of the constituent elements in an argon atmosphere. To obtain the homogenized samples, the alloys were heated at 1123 K for 3 days and then quenched in water. Powder specimens were obtained by grinding and annealed at 1123 K for 2 min to remove the induced strain. The phase characterization of the specimens was confirmed by X-ray powder diffraction measurements with using Cu- $K\alpha$ radiation. The dc magnetization measurements were carried out with using a commercial superconducting quantum interference device magnetometer. ^{57}Fe Mössbauer spectroscopy measurements were carried out in the 80 to 312 K temperature range in transmission geometry using a conventional spectrometer with a ^{57}Co -Rh source. Fittings with the obtained spectra were performed with *MossWinn* 3.0 program (Klencsár, Z.: Budapest, Hungary).

3. Results and Discussion

Figure 1 indicates phase diagram of Fe substituted $\text{Ni}_2\text{Mn}_{1.48-x}\text{Fe}_x\text{Sn}_{0.52}$ alloys reported by Fukushima *et al.* [13]. In the figure, A and M indicate the austenite and martensite phases, respectively, and T_C and T_C' indicate the Curie temperature, T_C , of the austenite phase and the martensite phase, respectively. T_{Ms} means the martensitic transformation starting temperature during cooling process. T_C slightly increases with increasing the Fe concentration, whereas T_{Ms} drastically decreases. In the figure, PM and FM mean paramagnetic and ferromagnetic states, respectively. It has been commonly thought that the martensitic transformation temperature, T_M , is significantly sensitive to the concentration and the behavior is explained as a function of the number of the valence electrons per atoms, e/a , namely, T_{Ms} increases with increasing e/a [16,17]. The explanation has been known to be a general rule to indicate the behavior of T_{Ms} of the Ni-based FSMAs. However, it has been recently reported that this rule does not hold when Fe is substituted for Mn in Ni_2MnGa [12,22,23]. Here, valence electrons of Fe is larger than that of Mn, thus, the Fe substitution for Mn means an increase of e/a . Such a break has also been observed in Ni-Mn-Sn alloys as shown in the Figure 1 [13]. Again, the experimental facts throw a question of an origin of the martensitic transformation, MT. The dashed

lines in the Figure mean the Fe composition of $x = 0.02, 0.04$ and 0.08 , they are the ^{57}Fe compositions that the Mössbauer spectroscopy measurements were performed in the present study in order to investigate the microscopic magnetic properties, where ^{57}Fe is doped instead of the normal Fe element in the $\text{Ni}_2\text{Mn}_{1.48-x}\text{Fe}_x\text{Sn}_{0.52}$ alloys.

Figure 1. Phase diagram of Fe substituted $\text{Ni}_2\text{Mn}_{1.48}\text{Sn}_{0.52}$ alloys reported by Fukushima *et al.* [13]. A and M indicate the austenite and martensite phases, respectively. T_C and T_C' indicate the Curie temperature of the austenite phase and the martensite phase, respectively. T_{Ms} means the martensitic transformation starting temperature during cooling process. PM and FM mean paramagnetic and ferromagnetic states, respectively.

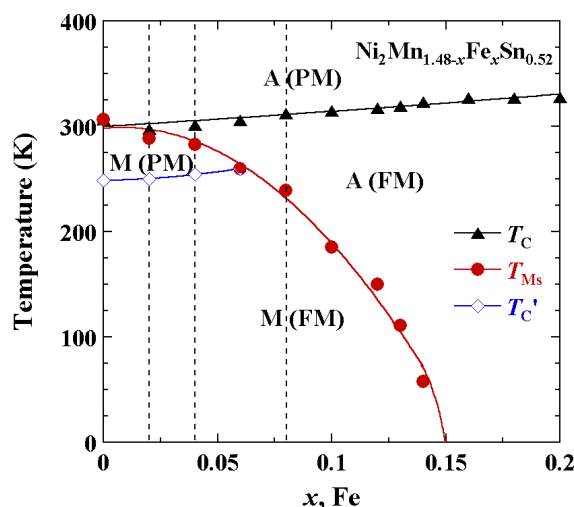
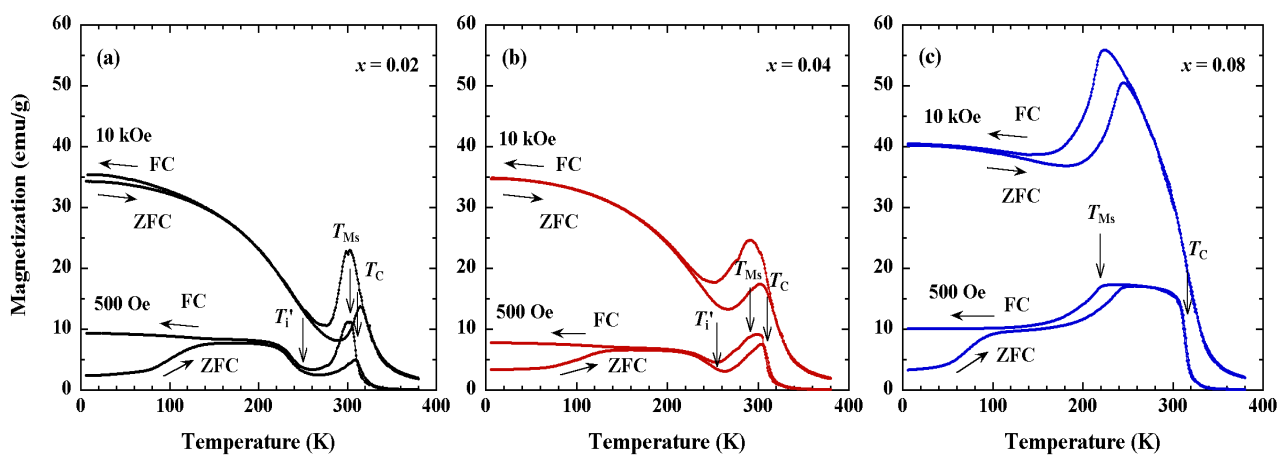


Figure 2. Thermomagnetization (M - T) curves measured under the magnetic fields of 500 Oe and 10 kOe for ^{57}Fe doped $\text{Ni}_2\text{Mn}_{1.48-x}\text{Fe}_x\text{Sn}_{0.52}$ ($x = 0.02, 0.04$ and 0.08) alloys. M - T curve for $x = 0.02$ at 500 Oe is same as the reported previously [10]. The arrows with ZFC and FC along the curves in (a), (b) and (c) show the zero-field-cooling and field-cooling processes, respectively.

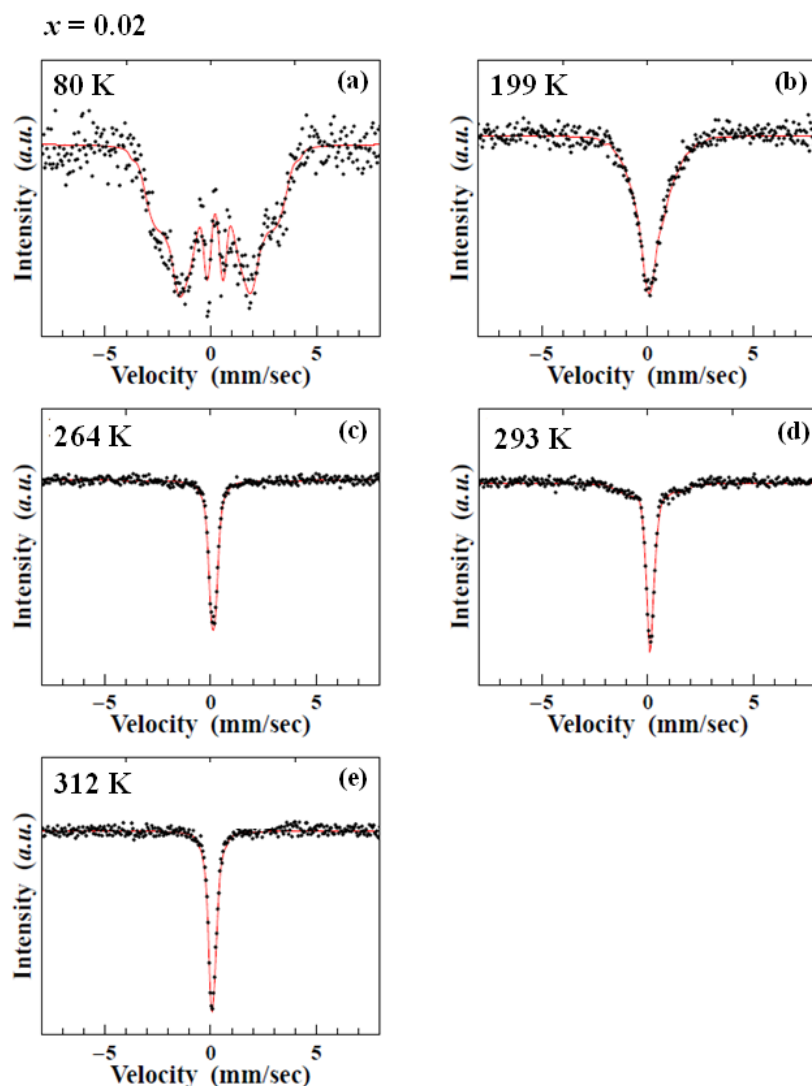


Thermomagnetization (M - T) curves measured under the magnetic fields of 500 Oe and 10 kOe for ^{57}Fe -doped $\text{Ni}_2\text{Mn}_{1.48-x}\text{Fe}_x\text{Sn}_{0.52}$ alloys with $x = 0.02, 0.04$ and 0.08 are indicated in Figure 2a–c, respectively. Here, M - T curve of $x = 0.02$ measured at 500 Oe is the same as the reported one [10].

From the M - T curves, it is shown that the magnetic transformation from the ferromagnetic to paramagnetic state in the austenite phase and MT occurs at almost the same time for $x = 0.02$. The temperature difference between T_C and T_{Ms} gradually expands with increasing ^{57}Fe content, being similar to the behavior indicated in the phase diagram in the Figure 1. That is, it is confirmed that the ^{57}Fe concentration dependence of T_C and T_{Ms} follows the phase diagram of the normal Fe-doped $\text{Ni}_2\text{Mn}_{1.48-x}\text{FeSn}_{0.5}$ system. The zero field-cooled (ZFC) and field-cooled (FC) M - T curves were measured during heating after the specimen was cooled down to low temperature in a zero applied magnetic field and during cooling in the applied magnetic field, respectively. In the all of the specimens for $x = 0.02$, 0.04 and 0.08, FC effects, that is, ZFC and FC curves do not coincide, are observed in low temperature range when the magnetic field is 500 Oe. T_i' is the temperature of the inflection point, and it is observed around 235 and 255 K for $x = 0.02$ and 0.04, respectively. In the phase diagram [13], although T_i' is treated as a magnetic transition temperature from the ferromagnetic state to the paramagnetic state in the martensite phase, the existence of the long-rang ferromagnetic ordering in the martensite phase is controversial even now. It will be discussed later. The value of T_C in the austenite phase, here T_C is defined as the temperature with showing the largest negative slope in the cooling M - T curve, was determined to be 309, 311 and 315 K for $x = 0.02$, 0.04 and 0.08, respectively, indicating tiny increase with increasing ^{57}Fe concentration. The values of T_{Ms} for $x = 0.02$, 0.04 and 0.08 confirmed by the M - T curves under 500 Oe are about 303, 300 and 220 K, respectively, being in good agreement with the phase diagram reported by Fukushima *et al.* [13].

The ^{57}Fe Mössbauer spectra taken at 80, 199, 264, 293 and 312 K for $x = 0.02$ and $x = 0.04$ are shown in Figure 3a–e [10] and in Figure 4a–e, respectively. Here, the measurement was performed at fixed temperatures in the heating process from 80 to 312 K. Whole of the aspects of the spectra are similar in both compositions. The spectra at 80 K of $x = 0.02$ in Figure 3a and of $x = 0.04$ in Figure 4a show a broad sextet arising from the wide distribution of hyperfine fields and the spectra at 199 K of $x = 0.02$ in Figure 3b and of $x = 0.04$ in Figure 4b exhibit a considerably wide line intensity distribution around maximum absorption due to the presence of the internal magnetic fields, indicating the existence of magnetic components. It should be noted that the magnetization on ZFC process shows a clear increase with increasing temperature up to around 200 K, while the magnetization on FC process indicates relatively plateau-like behavior under 500 Oe. Recently, ac susceptibility studies were performed and it was concluded that the magnetic feature of the ground state of $\text{Ni}_2\text{Mn}_{1.54}\text{Sn}_{0.46}$ alloy is magnetic blocking state because frequency dependence of the ac susceptibility is clearly observed, whereas no divergence in the non-linear term of the ac susceptibility is observed [24]. The magnetic properties of the ground state of the $\text{Ni}_2\text{Mn}_{1.54}\text{Sn}_{0.46}$ alloy are different from that of the $\text{Ni}_2\text{Mn}_{1.6}\text{Sb}_{0.4}$ alloy, which shows a negative peak in the non-linear ac susceptibility. On the basis of the experimental results, it was concluded that the magnetic ground state of the $\text{Ni}_2\text{Mn}_{1.6}\text{Sb}_{0.4}$ alloy is spin-glass. Although the concentration of the specimens with $x = 0.02$ and 0.04 in this study are different from the $\text{Ni}_2\text{Mn}_{1.54}\text{Sn}_{0.46}$ alloy, the magnetic ground state of the specimens with $x = 0.02$ and 0.04 may be the blocking state.

Figure 3. ^{57}Fe Mössbauer spectra and their fitting curves for $x = 0.02$ ($\text{Ni}_2\text{Mn}_{1.46}\text{Fe}_{0.02}\text{Sn}_{0.52}$) measured at 80, 199, 264, 293 and 312 K [10].



The spectra of 312 and 264 K in Figure 3c,d, in Figure 4c,d, are composed of a singlet with a narrow line width, while those at 293 K in Figure 3d and Figure 4d include a weak and broad sub-spectrum around the base of the sharp singlet, indicating the coexistence of magnetically ordered and disordered phases. From the M - T curves in Figure 2a,b, the specimens at 293 K for both $x = 0.02$ and $x = 0.04$ are seemed to be in a coexistent state with the martensite phase and the austenite phase. As shown in Figure 3c,e, and Figure 4c,e, both full widths at half maximum of the singlet spectra at 312 K and 264 K are almost equal in $x = 0.02$ and $x = 0.04$. The result means that the hyperfine field distribution of the spectrum taken from the nonmagnetic martensite phase at 264 K is almost the same as that from the paramagnetic austenite state at 312 K. It is strongly suggested that the martensite phase is paramagnetic in the temperature region just below T_M , and the paramagnetic region also exists for the specimen with $x = 0.04$. The paramagnetic and the ferromagnetic components in the spectra at 293 K will be brought from the paramagnetic martensite and ferromagnetic austenite phases. On the other hand, the spectra at 199 K become broader and the spectra at 80 K suggest the existence of the hyperfine field. As mentioned above, the FC effect is observed in the low temperature region for the

specimens with $x = 0.02$ and 0.04 . Concluding the results of the ac susceptibility measurements for the $\text{Ni}_2\text{Mn}_{1.54}\text{Sn}_{0.46}$ alloy [24], the magnetic state below T_1' would be blocking-state or spin glass-like state. Further study is needed to confirm whether the magnetically ordered state exists or not.

Figure 4. ^{57}Fe Mössbauer spectra and their fitting curves for $x = 0.04$ ($\text{Ni}_2\text{Mn}_{1.44}\text{Fe}_{0.04}\text{Sn}_{0.52}$) measured at 80, 199, 264, 293 and 312 K.

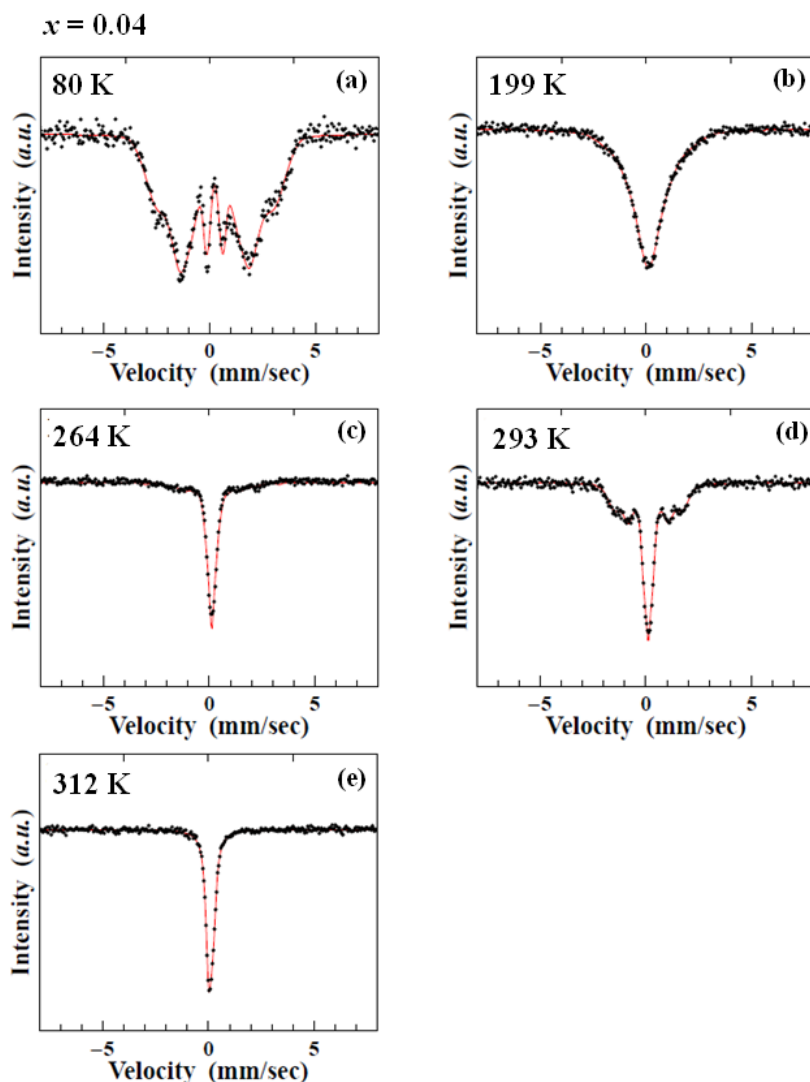
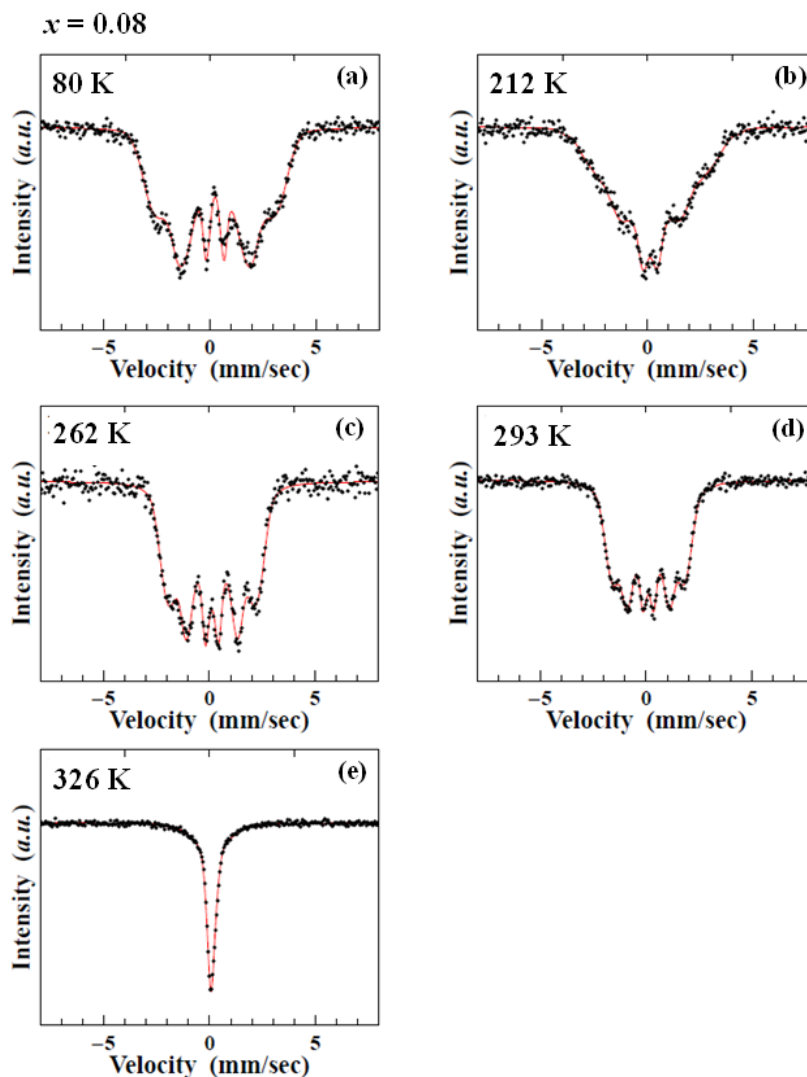


Figure 5a–e are ^{57}Fe Mössbauer spectra and their fitting curves for $x = 0.08$ ($\text{Ni}_2\text{Mn}_{1.40}\text{Fe}_{0.08}\text{Sn}_{0.52}$) measured at 80, 212, 262, 293 and 326 K, respectively. Although the aspects of the spectra at the each temperature of the specimens with $x = 0.02$ and 0.04 are similar, the spectra for $x = 0.08$ seem to differ from them. Spectrum of the singlet type is observed at only 326 K and it is due to the paramagnetism of the austenite phase from the result of the M - T curves in the Figure 2c, in where T_C is found to be about 315 K. On the other hand, sextet-like behavior is observed in the spectra measured at 262 and 293 K, and these are associated with the ferromagnetism in the austenite phase because the reverse T_M is about 200 K for $x = 0.08$ (See the Figure 2c). The spectra at 80 K and 212 K are also very broad and exhibit a wide distribution of hyperfine field. A distinct feature of the spectra at 80 K is that this shows an almost symmetric pattern in spite of the existence of electric quadrupole interactions. The

symmetric pattern of the spectra may be attributed to the blocking of iron moments in random directions to the axis of the electric field gradient.

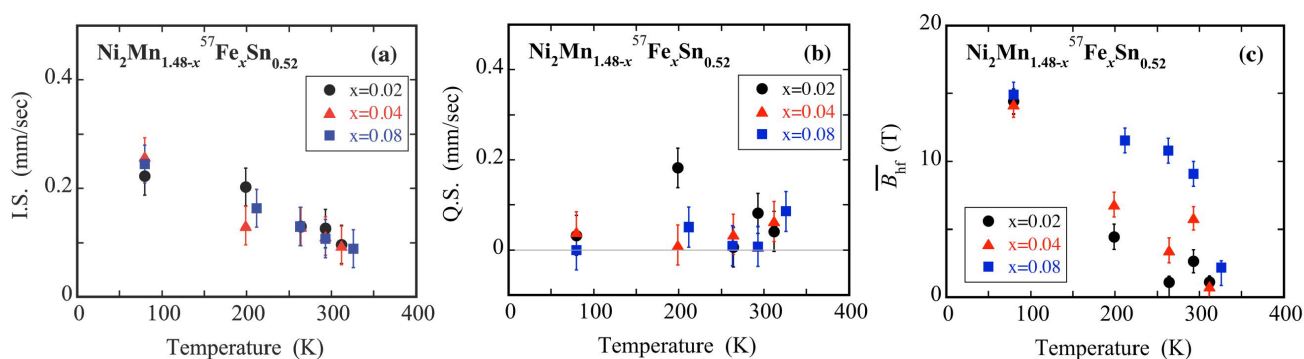
Figure 5. ^{57}Fe Mössbauer spectra and their fitting curves for $x = 0.08$ ($\text{Ni}_2\text{Mn}_{1.40}\text{Fe}_{0.08}\text{Sn}_{0.52}$) measured at 80, 212, 262, 293 and 326 K.



The temperature dependences of the isomer shift, I.S., the quadrupole splitting, Q.S., and the absolute average value of the ^{57}Fe hyperfine field, \bar{B}_{hf} , obtained by fitting for ^{57}Fe -doped $\text{Ni}_2\text{Mn}_{1.48-x}\text{Fe}_x\text{Sn}_{0.52}$ with $x = 0.02, 0.04$ and 0.08 are shown in Figure 6a–c. The I.S. shows monotonic decreases with increasing temperature for all specimens, and no composition dependence is observed. Because the I.S. relates to the position of the nuclei and the charge density, the monotonic behavior as a function of the temperature in this case is natural. In addition, concentration dependence of Q.S. is also not sensitive. In general, Q.S. reflects the symmetry of the crystal, with including the meaning of the magnetic configuration. The absolute values of Q.S. are comparatively small in the whole temperature range. It has been reported that the structure of the martensite phase of $\text{Ni}_2\text{Mn}_{1.44}\text{Fe}_{0.04}\text{Sn}_{0.52}$ is four-layered orthorhombic (4O) structure [12] and the symmetry of the crystal in the martensite phase becomes lower than that of the $L2_1$ -type cubic structure in the austenite phase. Although the value of the Q.S. for $x = 0.02$ at 199 K is somewhat distributed, there is a trend that the

absolute value of the Q.S. in the austenite phase may be slightly larger than those in the martensite phase. These behaviors, such as the monotonic decrease of I.S. with the temperature and slight change of the Q.S. between the martensite phase and austenite phase, have been also reported in ^{57}Fe -doped $\text{Ni}_2\text{Mn}_{1-x}\text{Fe}_x\text{Ga}$ alloys [25]. Such a comparatively small absolute values of the Q.S. in the martensite phase, even though the structure of the martensite phase has lower symmetry, would also be correlated to the magnetic state of the martensite phase. It has been reported from the studies of the ac magnetic susceptibility that the magnetic state of $\text{Ni}_2\text{Mn}_{1.54}\text{Sn}_{0.46}$ alloy in the martensite phase is blocking-state [24]. This may mean that the magnetic configuration of the blocking-state, where the magnetic spins are frozen to direct randomly, is rather symmetric than the magnetic state of the certain magnetic ordering with low symmetric structure. As shown in Figure 6c, the values of \bar{B}_{hf} at 80 K for all specimens are found to be about 15 T.

Figure 6. Temperature dependences of the isomer shift, I.S., the quadrupole splitting, Q.S., and the absolute average ^{57}Fe hyperfine field, \bar{B}_{hf} , obtained from the fitting in Figures 3–5.



It has long been known that the hyperfine fields, B_{hf} , at Fe nuclei in a lot of kinds of alloys containing Fe atoms is roughly proportional to the magnetic moments of Fe atoms with the coupling constant of $15 \text{ T}/\mu_{\text{B}}$. The values of \bar{B}_{hf} at Fe nuclei for $\text{Ni}_2\text{Mn}_{1.48-x}\text{Fe}_x\text{Sn}_{0.52}$ alloys in this study are much smaller than that expected from the coupling constant of $15 \text{ T}/\mu_{\text{B}}$. Similar phenomena were observed in $\text{Ni}_2\text{Mn}_{1-x}\text{Fe}_x\text{Ga}$ FSMA [25]. More recently, Umetsu *et al.* found from the neutron powder diffraction measurements that the magnetic moment of Fe atoms for $\text{Ni}_2\text{Mn}_{0.3}\text{Fe}_{0.7}\text{Ga}$ is about $3 \mu_{\text{B}}$ [26]. On the other hand, the values of \bar{B}_{hf} in the temperature range above 200 K for $x = 0.02$ and 0.04 are very small compared to those of $x = 0.08$. It is not clear why the large difference of the values of \bar{B}_{hf} for the specimens with $x = 0.02$, 0.04 and 0.08 appears above 200 K.

In this study, we confirmed that the magnetic state just below T_{M} of the specimens with $x = 0.02$ and 0.04 is paramagnetic from the Mössbauer spectroscopy measurements. The magnetic-field-induced reverse MT observed in Ni-Mn-Sn FSMA may be attributed to the large difference of magnetization between the paramagnetic martensite phase and the ferromagnetic austenite phase. In the Ni-Mn-Sn FSMA, there is some information in the literature on the giant magnetocaloric effect [27,28]. The origin of the giant magnetocaloric effect would be caused by the large entropy change between the paramagnetic martensite phase and the ferromagnetic austenite phase. As mentioned above, the number of the valence electrons per atom, e/a , is closely related to T_{M} : a large e/a indicates a higher T_{M} . However, such a correlation breaks down for the $\text{Ni}_2\text{Mn}_{1.48-x}\text{Fe}_x\text{Sn}_{0.52}$ and $\text{Ni}_2\text{Mn}_{1-x}\text{Fe}_x\text{Ga}$

FSMAs [12]. More detailed studies for the role of Fe atoms on the MT will be necessary to understand the mechanism of MT.

4. Summary

In order to investigate the Fe substitution effects on the magnetic properties of the Ni-Mn-Sn metamagnetic shape memory alloys, magnetic measurements and the Mössbauer spectroscopy experiments were carried out with using ^{57}Fe -doped specimens of $\text{Ni}_2\text{Mn}_{1.48-x}\text{Fe}_x\text{Sn}_{0.52}$ ($x = 0.02, 0.04$ and 0.08). Singlet-type Mössbauer spectra were clearly observed for $x = 0.02$ and 0.04 just below the martensitic transformation temperature, T_M , and above the Curie temperature, T_C , in the austenite phase. It was clear that the paramagnetic region exists just below T_M in the martensite phase for the specimens with $x = 0.02$ and 0.04 . In $\text{Ni}_2\text{Mn}_{1.48-x}\text{Fe}_x\text{Sn}_{0.52}$, T_C in the austenite phase slightly increases with increasing ^{57}Fe content; however, T_M significantly decreases. As a result, paramagnetic region is not observed in the martensite phase for $x = 0.08$, that is, martensite phase with small spontaneous magnetization directly transforms to the ferromagnetic austenite phase during heating. These results obtained from the Mössbauer spectra are consistent with the results of the magnetic measurements in this study and the phase diagram reported by Fukushima *et al.* for the normal Fe-doped $\text{Ni}_2\text{Mn}_{1.48-x}\text{Fe}_x\text{Sn}_{0.52}$ alloys [13]. As shown in the present results, the phase diagram for $\text{Ni}_2\text{Mn}_{1.48-x}\text{Fe}_x\text{Sn}_{0.52}$ breaks down the general rule for T_M versus the number of the valence electrons per atoms, e/a , which is common to the $\text{Ni}_2\text{Mn}_{1-x}\text{Fe}_x\text{Ga}$ alloys. Investigations of the role of Fe atoms in the magnetic properties for Ni_2MnGa and Ni-Mn-Sn FSMAs will be very important to clarify the mechanism of the martensitic transformation of these Ni-based ferromagnetic shape memory alloys.

Acknowledgments

The authors would like to thank H. Onodera for helpful discussion. This work was partly supported by a grant based on the High-Tech Research Center Program for private universities from the Japan Ministry of Education, Culture, Sports, Science and Technology (MEXT). This work was also partly supported by a Grant-in-Aid for Scientific Research, provided by the Japan Society for the Promotion of Science. Parts of this work were performed at the Center for Low Temperature Science, Institute for Materials Research, Tohoku University.

References

1. Ullakko, K.; Huang, J.K.; Kantner, C.; O'Handley, R.C.; Kokorin, V.V. Large magnetic-field-induced strains in Ni_2MnGa single crystals. *Appl. Phys. Lett.* **1996**, *69*, 1966.
2. Sozinov, A.; Likhachev, A.A.; Lanska, N.; Ullakko, K. Giant magnetic-field-induced strain in NiMnGa seven-layered martensitic phase. *Appl. Phys. Lett.* **2002**, *80*, 1746.
3. Webster, P.J.; Ziebeck, K.R.A.; Town, S.L.; Peak, M.S. Magnetic order and phase-transformation in Ni_2MnGa . *Phil. Mag. B* **1984**, *49*, 295.
4. Brown, P.J.; Kanomata, T.; Matsumoto, M.; Neumann, K.-U.; Ziebeck, K.R.A. *Magnetism and Structure in Functional Materials*; Planes, A., Mañosa, L., Saxena, A., Eds.; Springer-Verlag: Berlin Heidelberg, Germany, 2005; Chapter 7.

5. Entel, P.; Buchelnikov, V.D.; Khovailo, V.V.; Zayak, A.T.; Adeagbo, W.A.; Gruner, M.E.; Herper, H.C.; Wassermann, E.F. Modelling the phase diagram of magnetic shape memory Heusler alloys. *J. Phys. D Appl. Phys.* **2006**, *39*, 865.
6. Sutou, Y.; Imano, Y.; Koeda, N.; Omori, T.; Kainuma, R.; Ishida, K.; Oikawa, K. Magnetic and martensitic transformations of NiMnX(X = In,Sn,Sb) ferromagnetic shape memory alloys. *Appl. Phys. Lett.* **2004**, *85*, 4358.
7. Kainuma, R.; Imano, Y.; Ito, W.; Sutou, Y.; Morito, H.; Okamoto, S.; Kitakami, O.; Oikawa, K.; Fujita, A.; Kanomata, T.; *et al.* Magnetic-field-induced shape recovery by reverse phase transformation. *Nature* **2006**, *439*, 957.
8. Umetsu, R.Y.; Ito, K.; Ito, W.; Koyama, K.; Kanomata, T.; Ishida, K.; Kainuma, R. Kinetic arrest behavior in martensitic transformation of NiCoMnSn metamagnetic shape memory alloy. *J. Alloys Compds.* **2011**, *509*, 1389–1393.
9. Yu, S.Y.; Ma, L.; Liu, G.D.; Liu, Z.H.; Chen, J.L.; Cao, Z.X.; Wu, G.H.; Zhang, B.; Zhang, X.X. Magnetic field-induced martensitic transformation and large magnetoresistance in NiCoMnSb alloys. *Appl. Phys. Lett.* **2007**, *90*, 242501.
10. Umetsu, R.Y.; Kainuma, R.; Amako, Y.; Taniguchi, Y.; Kanomata, T.; Fukushima, K.; Fujita, A.; Oikawa, K.; Ishida, K. Mössbauer study on martensite phase in Ni₅₀Mn_{36.5}⁵⁷Fe_{0.5}Sn₁₃ metamagnetic shape memory alloy. *Appl. Phys. Lett.* **2008**, *93*, 042509.
11. Khovaylo, V.V.; Kanomata, T.; Tanaka, T.; Nakashima, M.; Amako, Y.; Kainuma, R.; Umetsu, R.Y.; Morito, H.; Miki, H. Magnetic properties of Ni₅₀Mn_{34.8}In_{15.2} probed by Mössbauer spectroscopy. *Phys. Rev. B* **2009**, *80*, 144409.
12. Kikuchi, D.; Kanomata, T.; Yamaguchi, Y.; Nishihara, H.; Koyama, K.; Watanabe, K. Magnetic properties of ferromagnetic shape memory alloys Ni₂Mn_{1-x}Fe_xGa. *J. Alloys Comd.* **2004**, *383*, 184.
13. Fukushima, K.; Sano, K.; Kanomata, T.; Nishihara, H.; Furutani, Y.; Shishido, T.; Ito, W.; Umetsu, R.Y.; Kainuma, R.; Oikawa, K.; *et al.* Phase diagram of Fe-substituted Ni-Mn-Sn shape memory alloys. *Scripta Mater.* **2009**, *61*, 813–816.
14. Xin, Y.; Li, Y.; Chai, L.; Xu, H. Shape memory characteristics of dual-phase Ni–Mn–Ga based high temperature shape memory alloys. *Scripta Mater.* **2007**, *57*, 599.
15. Wu, Z.; Liu, Z.; Yang, H.; Liu, Y.; Wu, G.; Woodward, R.C. Metallurgical origin of the effect of Fe doping on the martensitic and magnetic transformation behaviours of Ni₅₀Mn_{40-x}Sn₁₀Fe_x magnetic shape memory alloys. *Intermetallics* **2011**, *19*, 445.
16. Chernenko, V.A.; Pons, J.; Seguí, C.; Cesari, E. Premartensitic phenomena and other phase transformations in Ni–Mn–Ga alloys studied by dynamical mechanical analysis and electron diffraction. *Acta Mater.* **2002**, *50*, 53.
17. Chernenko, V.A. Compositional instability of β-phase in Ni-Mn-Ga alloys. *Scripta Mater.* **1999**, *40*, 523.
18. Lanska, N.; Söderberg, O.; Sozinov, A.; Ge, Y.; Ullakko, K.; Lindroos, V.K. Composition and temperature dependence of the crystal structure of Ni–Mn–Ga alloys. *J. Appl. Phys.* **2004**, *95*, 8074.
19. Krenke, T.; Acet, M.; Wassermann, E.F.; Moya, X.; Mañosa, L.; Planes, A. Martensitic transitions and the nature of ferromagnetism in the austenitic and martensitic states of Ni-Mn-Sn alloys. *Phys. Rev. B* **2005**, *72*, 014412.

20. Krenke, T.; Acet, M.; Wassermann, E.F.; Moya, X.; Mañosa, L.; Planes, A. Ferromagnetism in the austenitic and martensitic states of Ni-Mn-In alloys. *Phys. Rev. B* **2006**, *73*, 174413.
21. Han, Z.D.; Wang, D.H.; Zhang, C.L.; Xuan, H.C.; Zhang, J.R.; Gu, B.X.; Du, Y.W. The phase transitions, magnetocaloric effect, and magnetoresistance in Co doped Ni–Mn–Sb ferromagnetic shape memory alloys. *J. Appl. Phys.* **2008**, *104*, 053906.
22. Liu, Z.H.; Zhang, M.; Wang, W.Q.; Wang, W.H.; Chen, J.L.; Wu, G.H.; Meng, F.B.; Liu, H.; Liu, Y.B.D.; Qu, J.P.; *et al.* Magnetic properties and martensitic transformation in quaternary Heusler alloy of NiMnFeGa. *J. Appl. Phys.* **2002**, *92*, 5006.
23. Soto-Parra, D.E.; Moya, X.; Mañosa, L.; Planes, A.; Flores-Zúñiga, H.; Alvarado-Hernández, F.; Ochoa-Gamboa, R.A.; Matutes-Aquino, J.A.; Ríos-Jara, D. Fe and Co selective substitution in Ni₂MnGa: Effect of magnetism on relative phase stability. *Philos. Mag.* **2010**, *90*, 2771–2792.
24. Umetsu, R.Y.; Fujita, A.; Ito, W.; Kanomata, T.; Kainuma, R. Determination of the magnetic ground state in the martensite phase of Ni–Mn–Z (Z = In, Sn and Sb) off-stoichiometric Heusler alloys by nonlinear AC susceptibility. *J. Phys. Condens. Matter.* **2011**, *23*, 326001.
25. Amako, Y.; Taniguchi, Y.; Magatani, K.; Kikuchi, D.; Nakashima, M.; Kanomata, T. Mössbauer study on ferromagnetic shape memory alloys Ni₂Mn_{1-x}Fe_xGa. *J. Alloys Compds.* **2009**, *488*, 243.
26. Umetsu, R.Y.; Kikuchi, D.; Koyama, K.; Watanabe, K.; Yamaguchi, Y.; Kainuma, R.; Kanomata, T. Site occupancy and magnetic moment of Fe in the Ni₂Mn_{0.3}Fe_{0.7}Ga alloy by neutron powder diffraction study. *J. Alloys Compd.*, submitted for publication, 2013.
27. Krenke, T.; Duman, E.; Acet, M.; Wassermann, E.F.; Moya, X.; Manosa, L.; Planes, A. Inverse magnetocaloric effect in ferromagnetic Ni-Mn-Sn alloys. *Nature Mater.* **2005**, *4*, 450.
28. Han, Z.D.; Wang, D.H.; Zhang, C.L.; Xuan, H.C.; Gu, B.X.; Du, Y.W. Low-field inverse magnetocaloric effect in Ni_{150-x}Mn_{39+x}Sn₁₁ Heusler alloys. *Appl. Phys. Lett.* **2007**, *90*, 042507.

© 2013 by the authors; licensee MDPI, Basel, Switzerland. This article is an open access article distributed under the terms and conditions of the Creative Commons Attribution license (<http://creativecommons.org/licenses/by/3.0/>).